Chapter 13
A Perspective on the Particle-Based Crystal Growth of Ferric Oxides, Oxyhydroxides, and Hydrous Oxides

R. Lee Penn, Dongsheng Li, and Jennifer A. Soltis

13.1 Introduction

The diversity of iron oxide, oxyhydroxide, and hydroxide materials in natural settings is remarkable. Hereafter referred to simply as the iron oxides, these materials exhibit myriad textures and morphologies, and such features provide evidence that classical growth cannot adequately explain the formation and growth of iron oxides.

The iron oxides often form as a result of iron leaching from iron-containing minerals (e.g., biotite) through both abiotic and biotic weathering processes (Barker et al. 1998). Furthermore, iron oxides can form when natural water containing Fe(II) encounters oxidizing conditions (e.g., Waychunas et al. 2005). With its abundance in near-surface materials and its redox reactivity, iron plays important roles in biogeochemical cycling of a wide range of species, including metals and molecular species. The capacity of the iron oxides for sorption of metals and polyatomic anions makes these materials important players in the fate and transport of a wide range of contaminants (Waychunas et al. 2005). Elucidating how these minerals form, transform, aggregate, and grow is critical to understanding their geochemical reactivity.

Particle-based crystallization has been featured prominently in the recent crystal growth literature (De Yoreo et al. 2015 and references therein). Of the diverse crystal growth mechanisms known, both classical crystal growth and particle-based crystal growth are particularly important in the iron oxides. Classical crystal growth

R.L. Penn (✉) • J.A. Soltis
Department of Chemistry, University of Minnesota, 207 Pleasant St SE, Minneapolis, MN 55455, USA
e-mail: rleepenn@umn.edu

D. Li
Pacific Northwest National Laboratory, 902 Battelle Boulevard, Richland, WA 99352, USA

A.E.S. Van Driessche et al. (eds.), *New Perspectives on Mineral Nucleation and Growth*,
DOI 10.1007/978-3-319-45669-0_13

can be simply described as the monomer-by-monomer addition of molecular-scale species to a growing crystal. Oriented attachment is a special case of particle-based crystal growth and has been recognized since at least the late nineteenth century (Ivanov et al. 2014). In oriented attachment, primary particles associate to reversibly form complexes that are analogous to the outer sphere complexes described in inorganic chemistry. The primary particles composing these complexes lack direct contact, with solvent molecules and other molecular-scale species residing in the spaces separating them. The primary particles can rearrange and reorient through Brownian motion within this intermediate structure. If the primary particles achieve a common crystallographic orientation, the intermediate structures, which are sometimes referred to as mesocrystals (Cölfen and Mann 2003; Yuwono et al. 2010; Rao and Cölfen 2017, Chap. 8), can either dissociate or irreversibly bond together to form new secondary crystals. These new crystals can have symmetry-defying morphologies and contain defects like dislocations, stacking faults, and twin boundaries (Penn 2004).

Numerous reviews describing crystal growth by oriented attachment have appeared in the relatively recent literature (De Yoreo et al. 2015; Ivanov et al. 2014; Xiong and Tang 2012; Dalmaschio et al. 2010; Zhang et al. 2010; Zhang et al. 2009; Niederberger and Cölfen 2006; Penn 2004), among others. These reviews provide concise descriptions of the fundamental mechanism as well as observations of oriented attachment, reporting numerous examples of oriented attachment in synthetic materials, such as titanium dioxide, iron oxides, metal selenides and sulfides, and more. In addition, evidence for oriented attachment (OA) has been observed in natural environment (Banfield et al. 2000; Hochella et al. 2008; Penn et al. 2001b).

Currently, there is no universal description of how the iron oxides grow. In fact, the iron oxides literature is rife with contradictions, even when observed morphologies, textures, and microstructures are similar. An excellent example is the case of pseudocubic hematite crystals, which have been prepared by several research groups. Kandori et al. (1991) prepared synthetic hematite by aging an acidic solution of ferric chloride at 100 °C for 20 days, and they described their product pseudocubic crystals as polycrystals composed of smaller and oriented subcrystals. They concluded that the pseudocubic hematite formed by aggregation of hydrous ferric oxide crystallites is followed by recrystallization and dehydration. Whether the hydrous ferric oxides precursor particles were oriented prior to recrystallization and dehydration was not addressed (Kandori et al. 1991). Similarly, Sugimoto et al. (1993) described their synthetic pseudocubic hematite particles, which were prepared by aging a partially neutralized solution of ferric chloride at 100 °C for 8 days, as consisting of oriented subcrystals and even stated that their product appeared similar to that of Kandori et al. (1991). However, they stated that single crystals could not be produced by an aggregative mechanism and concluded that their pseudocubic hematite must have grown by addition of monomeric species (e.g., dissolved ferric complexes) from the solution phase. They concluded that the observed textures arose because individual two-dimensional surface nuclei

could not progress to form a continuous surface layer due to surface sites blocked by adsorbed species like protons, chloride anions, and chloro ferric complexes (Sugimoto et al. 1993).

Texture, morphology, microstructure, and the absence or presence of defects can serve as clues regarding the crystal growth mechanisms at play. Relics of a particle-mediated crystal growth mechanism can include dimpled surfaces, symmetry-defying morphologies, dislocations, twin boundaries, stacking faults, and internal porosity, and many of these features are often observed in reports describing iron oxide crystal growth and phase transformations. Indeed, features apparent in images of iron oxide particles shown in the classic Cornell and Schwertmann (Cornell et al. 1989; Cornell and Schwertmann 2003) books are often consistent with particle-mediated crystal growth. Recent work has demonstrated the importance of aggregation, including oriented attachment, not only in iron oxide crystal growth (e.g., Burleson and Penn 2006; Burrows et al. 2012; Burrows et al. 2013; Penn et al. 2006) but also during iron oxide phase inter-transformations (e.g., Davidson et al. 2008; Frandsen et al. 2014). Aggregation, including the special case of oriented attachment, can lead to final crystals with rough surfaces as well as the incorporation of pore spaces, defects, stacking faults, all of which can dramatically impact the chemical and physical properties of the iron oxides.

Nucleation of particles with a structure distinct from the thermodynamically most stable phase given the conditions (e.g., pH, temperature) is also common. Phase transformation subsequently occurs to produce the more stable phase at the expense of the initially nucleated phase. An excellent example is goethite produced from six-line ferrihydrite nanoparticles in moderately acidic aqueous suspensions (e.g., Burleson and Penn 2006; Burrows et al. 2012; Burrows et al. 2013; Penn et al. 2006). Forced hydrolysis of dissolved ferric nitrate results in formation of ferrihydrite nanoparticles that are a few nanometers in diameter. With time, the ferrihydrite nanoparticles loosely aggregate into fractal aggregates, within which the primary particles rearrange and reorient to form linear strings of nanoparticles. These linear strings range from one to a few primary particles wide and several to tens of particles long. In this intermediate state, the primary particles lack direct contact with one another, with water and possibly other dissolved species residing in the spaces between them. Further, the fraction of particles residing in the linear strings increases with time (Yuwono et al. 2010), as does the fraction of goethite. At some point, the phase transformation from ferrihydrite to goethite occurs. Based on high-resolution imaging and X-ray diffraction results (Burleson and Penn 2006) in combination with high-resolution imaging of the loose aggregates in vitrified water (Yuwono et al. 2010), the current hypothesis is that phase transformation to goethite precedes rearrangement from random appearing fractal aggregates to linear strings of nanocrystals (Fig. 13.1 upper scheme). Indeed, linear strings with overall morphologies consistent with goethite twins were frequently observed (e.g., Fig. 13.2), with the angle between the crystalline arms residing on either side of the twin boundary matching that observed in twinned goethite crystals (Yuwono et al. 2010).

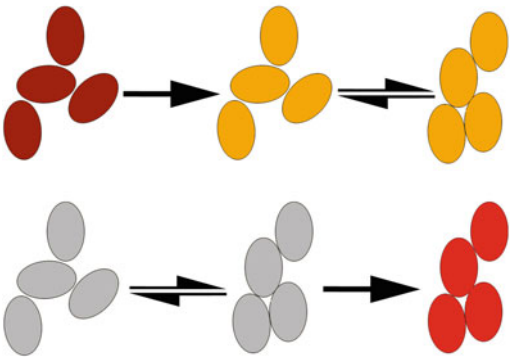

Fig. 13.1 Simple scheme illustrating the two end member possibilities for phase transformation after (*top*) or before (*bottom*) primary particles are crystallographically aligned with respect to one another

Fig. 13.2 Cryo-TEM image of aggregates of iron oxide nanoparticles. The aggregate with the shape of "v" has a morphology and size that matches those of goethite twins observed in the product material. High-resolution images of similar objects demonstrate lattice fringes that span the entire object and with spacings consistent with the goethite crystal structure (Yuwono et al. 2010)

Alternatively, the phase transformation could occur after a threshold size is achieved (Fig. 13.1 lower scheme). Indeed, size-dependent thermodynamic relationships between initial and product phases can mean that the new phase is not thermodynamically favored until the initially nucleated crystals reach a threshold size (Navrotsky et al. 2008). This results from the interplay between surface and bulk energies, with the material with lower surface energy favored at small size and the material with lower bulk energy favored at larger size. A beautiful example of phase transformation occurring after oriented attachment is hematite produced from oriented aggregates of akaganeite under hydrothermal conditions. Cryo-TEM, in combination with XRD results, leads to the proposal that akaganeite nanorods grew by oriented attachment and that the initial formation of hematite was driven by a change in phase stability due to the increasing size of the akaganeite crystallites. That is to say, once an akaganeite crystallite passed a threshold size, phase transformation was driven by the comparative stability of hematite versus akaganeite (Frandsen et al. 2014). Such size-dependent phase stability has been demonstrated in a number of systems, such as the titanium dioxides (Navrotsky 2011), calcium sulfate (Van Driessche et al. 2012), as well as the iron oxides system (Navrotsky et al. 2008).

In fact, considering the size-dependent phase stability of the iron oxides means reevaluation of the results presented above regarding the growth of goethite from

six-line ferrihydrite. Examining the thermodynamic relationships presented by Navrotsky et al. (2008) does not, unfortunately, yield a clear answer regarding the relative phase stability of ferrihydrite compared to goethite at extremely small particle size. Ferrihydrite presents unique challenges because its crystal structure, its hydrated state, and the probability that this material's composition may vary with particle size are not yet well understood. A challenge of the high-resolution transmission electron microscopy (HRTEM) images presented by Burleson and Penn (2006) is that the particles were dried before inserting into the high vacuum of the transmission electron microscope (TEM). Thus, conclusions drawn about the structure of individual particles as observed via HRTEM may not match the structure of individual particles while still suspended in aqueous solutions. Nevertheless, the relative stability for akaganeite and hematite as a function of particle size (Navrotsky et al. 2008) seems consistent with the conclusions described by Frandsen et al. (2014).

13.2 The Critical Role of Materials Characterization

Generally speaking, the final morphology, microstructure, and texture of a crystalline object are path dependent. That is to say, the detailed crystal growth mechanism leads to the presence and/or absence of specific features in the growing crystal. However, the dominant crystal growth mechanism(s) can change over time. Later crystal growth can effectively erase evidence for early crystal growth mechanisms (De Yoreo et al. 2015). The above disparate descriptions of how hematite crystals composed of smaller subcrystals form highlight the challenges of connecting the properties of the final product to its crystal growth history. Interestingly, Sugimoto et al. (1993) stated that drawing conclusions from ex situ TEM images is problematic because the dispersed state of the particles will change upon drying on the TEM grid. Indeed, drawing conclusions based on data obtained once the final crystal has been produced is risky, although sometimes these are the only data available (e.g., crystals formed long ago in natural environments). Thus, there is a pressing need for reliable characterization methods that can enable holistic determination of the path to a final crystal. The most robust approaches will combine methods, both in situ and ex situ, with particular focus on techniques that enable characterization as a function of time (Penn and Soltis 2014).

13.2.1 Imaging Using Transmission Electron Microscopy (TEM)

Direct imaging of nanoparticles using TEM and high-resolution TEM has long been the primary technique for characterizing the often nanoscale features typically associated with particle-based crystal growth mechanisms. Features such as crystal

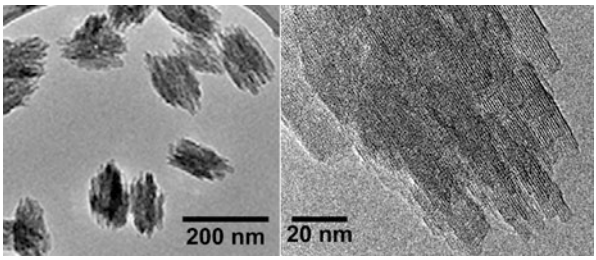

Fig. 13.3 TEM images of silicalite-1 prepared using bis-1,6-(tripropyalammonium)hexamethylene dihydroxide as the structure-directing agent. The sample was prepared after repeated washing and centrifugation to remove dissolved species and amorphous material from the aqueous suspension. The high-resolution image highlights the internal porosity and very complicated microstructure arising from aggregation of structural diverse precursor nanoparticles followed by recrystallization (Kumar et al. 2011)

twinning, dislocations, and dimpled boundaries can often be readily detected and even quantified in TEM images (Penn and Soltis 2014). However, detecting such features does not represent sufficient evidence for concluding a crystal has formed by oriented attachment or another particle-based growth mechanism. Indeed, features like dimples and twins could form by random particle attachment followed by recrystallization (Kumar et al. 2008; Kumar et al. 2011) (Fig. 13.3); alternatively, this can proceed by monomer-by-monomer growth onto surface nuclei that cannot extend beyond some physical or chemical barrier residing on the crystal surface, as hypothesized by Sugimoto et al. (1993). Likewise, the absence of such features is not a conclusive indicator of classical crystal growth, since rough surfaces and defects can essentially be erased when particle-based crystal growth is accompanied or followed by recrystallization or monomer-by-monomer crystal growth. It is therefore critical to employ correlative methods, time-resolved methods, and in situ methods like X-ray scattering and cryogenic TEM (Penn and Soltis 2014).

13.2.2 Cryogenic and Fluid Cell TEM

Cryogenic (cryo) and fluid cell TEM enable direct imaging of particles as they exist suspended in solvents (De Yoreo et al. 2017, Chap. 1; Nielsen and De Yoreo 2017, Chap. 18). This removes the potential for artifacts that can arise due to drying a sample on a TEM grid. The methods differ in that cryo-TEM provides a snapshot of the sample at the instant of cryogenic vitrification, while fluid cell TEM enables capture of the movement of particles in their suspended state. To prepare a sample for cryo-TEM, a thin film of suspension is applied to a TEM grid and then plunged into liquid cryogen (typically liquid ethane for aqueous suspensions) (Burrows and Penn 2013). The rapid cooling (ca. 100,000 K per second) achieved by plunging

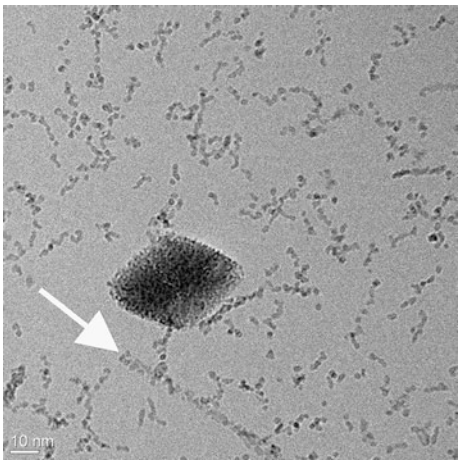

Fig. 13.4 Cryo-TEM image of an aqueous suspension of three types of iron oxide particles: (1) hematite (large *diamond-shaped* particle), (2) linear arrangements of primary particles with size and shape similar to goethite crystals produced by OA, and primary particles that are aggregated (3) or isolated (4). In the lower center of the field of view, the linear arrangement of particles is consistent with the size and shape of final goethite crystals (*white arrow*), and the working hypothesis is that the primary particles within that linear arrangement have the goethite crystal structure

into liquid cryogen ideally serves to preserve the arrangement of objects in the solvent and prevent crystallization of solvent molecules. By maintaining cryogenic conditions during imaging and minimizing the electron dose, one can obtain high-resolution images of crystals as they existed in the liquid state at the instant of vitrification. Figure 13.4 shows a cryo-TEM image of an aqueous suspension aged at 80 °C. Several different nanostructures can be discerned in this image: (1) a large crystal of hematite, with texture consistent with particle-mediated crystal growth; (2) an aggregate of particles with morphology, aspect ratio, and size consistent with product goethite crystals (arrow); (3) fractal aggregates with random orientation of primary particles, which are hypothesized to be ferrihydrite; and (4) isolated primary particles, which are also hypothesized to be ferrihydrite.

To prepare a sample for fluid cell TEM characterization, one need only ensure that the mass loading of particles is suitable for characterization. The two basic options are a static cell and a flow-through cell. An aliquot of suspension is injected into a static cell and the cell sealed, which means only a single aliquot of suspension can be examined with each cell. In the flow-through cell, the cell has both inlet and outlet, and fresh suspension can be flowed into the cell. Both cells are bounded by two electron-transparent windows (Grogan et al. 2012; Penn and Soltis 2014; Nielesen and de Yoreo 2017, Chap. 18). Either way, imaging by fluid cell TEM can yield unprecedented insights into the dynamics of particle-particle interactions, enabling quantitative characterization of particle motion, rearrangement of particles in loosely bound aggregates, crystal growth, and crystal dissolution. Generally

speaking, the thickness of the liquid layer is thinner for the static than for the flow-through cell, which means higher resolution and better contrast are obtained with the static cell.

De Yoreo and coworkers successfully captured an instance of oriented attachment between two ferrihydrite crystals in an aqueous solution (Li et al. 2012). They directly imaged two ferrihydrite crystallites moving in suspension. The ferrihydrite crystallites achieved close approach, and the authors were able to directly observe the particles rearranging with respect to one another. A particle-particle attachment occurred once crystallographic alignment was achieved, and continued crystal growth by coarsening immediately after the oriented attachment event was observed (Li et al. 2012). This resulted in smoothening out of the high radius of curvature dimples that formed upon oriented attachment (Li et al. 2012). In addition to quantifying the translational and rotational velocity of the smaller particle, they also quantified the rate of coarsening by measuring the rate at which the curved surfaces at particle-particle interfaces were eliminated. Their experimental rate of coarsening was consistent with the dependence of chemical potential on interface curvature (Cao 2004; Li et al. 2012).

The advantages of obtaining direct images of particles as they exist in liquid suspension by cryo and fluid cell TEM come with some serious challenges. As with all TEM methods, beam damage is a potential and serious complication. Both radiolysis and knock-on damage can result in substantive changes to samples during imaging. Unique to cryo-TEM, exposure to the beam can induce crystallization of the vitrified solvent, which can result in the introduction of diffraction contrast that can obscure the objects of interest. One main advantage of vitrification is that the amorphous solvent contributes a uniform background, which means that nanoparticles of sufficient size (with respect to the total thickness of the solvent film) can be readily discerned. In addition, the amorphous solvent can liquefy or sublime, which can cause the particles to move (Burrows and Penn 2013; Burrows et al. 2014). In fluid cell TEM, additional considerations are numerous (Ross 2015) and include the possibility that particles could interact with the cell windows, with irreversible adhesion to the cell window or modified particle-particle interactions both possibilities (Liu et al. 2013; Yuk et al. 2012; Zheng et al. 2009). Finally, exposure to a sufficiently intense beam can yield substantial reduction of Fe^{3+} to Fe^{2+} (Pan et al. 2006), which could result in the reductive dissolution of ferric oxide during imaging. Figure 13.5 shows a series of images of goethite crystals in water captured from a video collected while using a fluid cell TEM. Upon exposure to the beam (unquantified intensity), the ca. one to two hundred nanometer goethite crystals dissolved within approximately 70 s. Moving to a nearby location revealed that crystals not exposed to the beam remained intact and appeared unaltered, although onset of dissolution was observed soon after selecting a new field of view. Furthermore, under similar conditions in the laboratory, no detectable dissolution occurs. Thus, we conclude that the goethite reductively dissolved due to exposure to the electron beam (Fig. 13.5).

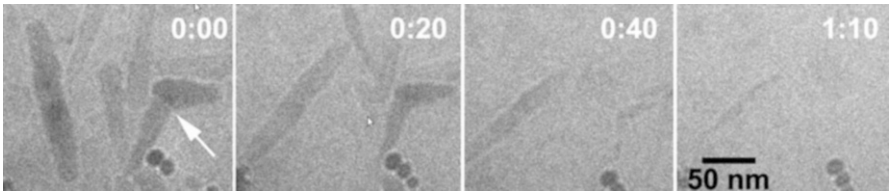

Fig. 13.5 Fluid cell TEM images obtained as snapshots from a video recording initiated immediately after the *left-hand*, acicular particles were in the field of view. The dark-appearing round objects are unknown contamination. The ca. 100–200 nm long by 20–50 nm wide particles are goethite crystals, and one twinned particle can be seen on the *right-hand* size of the time zero image (*large white arrow*). The ca. 200 nm long goethite crystal on the *left-hand* side of the field of view rotated as it dissolved

13.2.3 Correlative Methods

One major problem with the above TEM methods is vanishingly small amounts of material are imaged. In Fig. 13.5, the amount of material imaged in the left-most panel is a fraction of a femtogram. High-resolution micrographs typically involve just attograms of material. Thus, techniques that can produce data for comparatively bulk samples are essential to ensuring the data are suitably representative of the overall sample. X-ray diffraction (XRD) (Chiche et al. 2008; Hapiuk et al. 2013; Huang et al. 2003) and other diffraction techniques can be used to identify minerals and quantify crystallite size, size distribution, and morphology. Scattering techniques, such as small angle X-ray scattering (SAXS) (Davis et al. 2006; Drews and Tsapatsis 2007; Kumar et al. 2008; Stawski and Benning 2013), small angle neutron scattering (SANS) (Schwahn et al. 2007), and dynamic light scattering (DLS) (Davis et al. 2006; Mintova et al. 2002; Schwahn et al. 2007) can be used to quantify particle size and size distribution of particles in the suspended state. A more detailed description of some of these methods for characterizing growth via oriented attachment can be found in a review by Penn and Soltis (2014).

Kinetic models serve as an important method for detecting crystal growth by particle-based mechanisms, especially when more than one crystal growth mechanism operates. Several models employed for quantifying crystal growth that involves aggregative processes, including oriented attachment, have been reviewed elsewhere (Burrows et al. 2010; Xue et al. 2014), and describing those models is beyond the scope of this chapter. However, the addition of semiquantitative and quantitative models improves drastically our ability to detect crystal growth by particle-based mechanisms, even when features that could serve as indicators of such growth have been erased by subsequent processes.

13.3 Highlights of Particle-Mediated Crystal Growth in the Iron Oxides Literature

The work of Cornell and Schwertmann dramatically changed our understanding of the occurrence and formation of iron oxides. Their books (Cornell and Schwertmann 2003; Schwertmann and Cornell 2000; Cornell and Schwertmann 2006) feature descriptions of iron oxide minerals and reliable recipes for synthesizing them, complete with results from careful materials characterization. Below are some highlights of reports describing iron oxide crystal growth by nonclassical, particle-based mechanisms.

13.3.1 Goethite

Goethite (α-FeOOH) has been described as the dominant reactive iron oxyhydroxide in lake and marine sediments (van der Zee et al. 2003). Physical properties like microstructure, particle size, and aggregation state are expected to strongly impact the behavior of this ubiquitous and redox reactive material.

Evidence for goethite crystal growth by a particle-based mechanism was described in the 1970s. Murphy et al. (1976a) prepared synthetic goethite from partially neutralized solutions of ferric nitrate, and in their paper they describe goethite growth by spheres linking together to form rods. They describe the spheres as discrete, with sizes in the 1.5–3 nm size range and refer to them as polycations that initially form in the partially neutralized ferric nitrate solutions. In related work, they (Murphy et al. 1976b) describe goethite growth from ferric perchlorate solutions that also starts with spheres linking together to form rods. They again describe the spheres as polycations, which initially form in the ferric perchlorate solutions as discrete spheres in the 1.5–3 nm size range, and they further discuss link between ionic strength and rod formation. Whether their growth mechanism involves a phase transformation to goethite that precedes or follows the aggregation step is unclear.

Burleson and Penn (2006) proposed a two-step growth mechanism for goethite crystal growth under aqueous conditions. They suggested that primary particles first transformed from ferrihydrite to goethite followed by secondary assembly via oriented attachment (Burleson and Penn 2006). This hypothesis was supported by the cryo-TEM work published by Yuwono et al. (2010), in which images of loose aggregates composed of oriented goethite primary particles were presented. The kinetics of goethite growth by oriented attachment as well as the final goethite crystal size are sensitive to temperature and pH (Burleson and Penn 2006; Burrows et al. 2013), ionic strength (Burrows et al. 2012), precursor particle size (Penn et al. 2006; Penn et al. 2007), and the presence of chemical additives (Yuwono et al. 2012).

The aforementioned studies on goethite crystal growth were mainly performed at mildly acidic conditions. In contrast, Schwertmann and Murad (1983) performed experiments at higher pH, and they concluded that goethite had been formed by a dissolution and reprecipitation mechanism. No evidence for goethite growth by oriented attachment has been reported, and their general conclusion seems to be dissolution and precipitation dominates at high pH due to increased Fe(III) solubility (Davidson et al. 2008; Shaw et al. 2005).

13.3.2 Hematite

The case of the pseudocubic hematite is but one example of disparate interpretations based on very similar observed crystal textures. Similarly, spindle-shaped hematite particles consisting of oriented subcrystals have been described as growing by two different mechanisms. Morales et al. (1992) concluded that the spindle-shaped hematite was formed by an aggregation process involving hematite crystallites. In contrast, Sugimoto et al. (1993) stated that single crystals could not be constructed by aggregation of primary crystallites and concluded that these structures were formed by direct monomer-by-monomer addition of ferric complexes from the solution phase.

Bailey et al. (1993) used time-resolved TEM and cryo-TEM to examine the evolution of iron oxide particles produced from aqueous solutions of ferric chloride. They concluded that their 1.5 μm hematite nanocubes formed from raft-like aggregates of rod-shaped akaganeite nanoparticles aligned along <001>. They proposed that hematite nucleated within the structure of the raft-shaped oriented aggregate. Ocaña et al. (1995) described the "ordered aggregation" of small ellipsoidal hematite nanoparticles to form larger hematite crystals. Finally, Fischer and Schwertmann (1975) described the coalescence of "amorphous particles" into larger aggregates that eventually transform into single crystals of hematite (Fischer and Schwertmann 1975). Their results may be consistent with crystal growth by oriented attachment preceded by or followed by phase transformation from ferrihydrite to hematite.

Hematite produced by aging an acidic ferric chloride solution at elevated temperature exhibited a texture consistent with crystal growth by oriented attachment, resulting in the formation of lobed single crystals containing significant defects, such as edge dislocations (Penn et al. 2001a). In addition, the recent work of Frandsen et al. (2014) demonstrated hematite growth that indirectly involves crystal growth by oriented attachment. In their work, akaganeite crystals grew by oriented attachment, and the larger secondary crystals eventually phase transformed to hematite. Other examples of particle-based hematite growth undoubtedly exist.

13.3.3 Akaganeite

Akaganeite is a less common iron-bearing mineral that is not precisely an iron oxide mineral since it contains structural chloride. This mineral often occurs in the nanoscale size range and is often a precursor phase to the more stable hematite (e.g., Frandsen et al. (2014)). It has been described as occurring in the vicinity of biological organisms, with biological polymers serving to template the crystallization of akaganeite (Chan et al. 2004). It is less frequently studied (Barron and Torrent 2013), but the material frequently exhibits features that may indicate particle-mediated crystal growth.

An early report describing akaganeite crystal growth featured the conclusion that akaganeite grew from ferric chloride solutions by addition of subcrystals to produce the final larger structure. Watson et al. (1962) prepared ultrathin sections of akaganeite collected from aged solutions of ferric chloride (Fig. 13.6). Images of cross sections of their akaganeite crystals demonstrate that they are composed of oriented arrays of tetragonal prisms of crystalline akaganeite.

Similar to their work with goethite, Murphy et al. (1976c) described akaganeite growth from partially neutralized solutions of ferric chloride, starting with spheres that link together to form rods. They described the initial spheres as polycations that are in the 1.5–3 nm size range. Whether their growth mechanism involves a phase transformation to goethite that precedes or follows the aggregation step is once again (and understandably) unclear.

Recent work by Frandsen et al. (2014), which is described above, demonstrates akaganeite crystal growth by oriented attachment, using cryo-TEM tomography to produce exquisite three-dimensional images of the crystals.

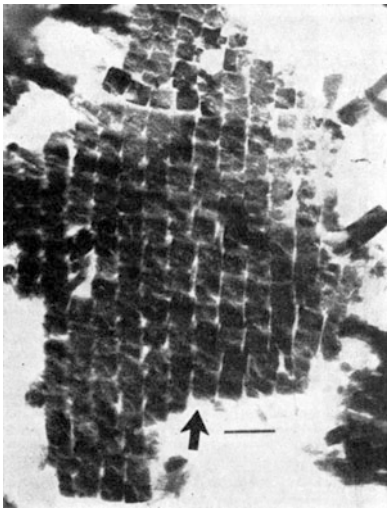

Fig. 13.6 TEM image of a cross-sectional ultra thin section of an akaganeite crystal impregnated with polymethracrylate. The scale bar represents 100 nm. High-resolution images of the individual tablets confirms their crystalline nature as well as the parallel crystallographic alignment (Watson et al. 1962)

13.3.4 Feroxyhite

Feroxyhite (δ-FeOOH) nanocrystals, which were produced upon oxidation of an Fe(II)-bearing precipitate prepared by neutralizing a solution of ferrous chloride, were described as high aspect ratio particles, with substantial dimpling, porosity, and incorporation of defects like edge dislocations. The authors concluded that the feroxyhite crystals had formed by oriented attachment (Penn et al. 2001a).

13.3.5 Ferrihydrite

Ferrihydrite is in a class of its own. There is a lack of consensus regarding its crystal structure, homogeneity, and even composition (Drits et al. 1993; Gilbert et al. 2013; Janney et al. 2000, 2001; Michel et al. 2007). This iron oxyhydroxide occurs only as nanoparticles, with sizes typically ranging from one to several nanometers, and its structure continues to be poorly understood. This material is often the first solid material to form upon partial neutralization of solutions containing ferric ions, and it is often prepared as a precursor to the more thermodynamically stable iron oxides like goethite and hematite (e.g., Cornell et al. 1989; Cornell and Schwertmann 2003, 2006). In fact, aqueous suspensions containing ferrihydrite nanoparticles typically are not stable, with the more stable iron oxide minerals, such as goethite and hematite, forming even after quite short aging times. The new phases often exhibit textures and morphologies consistent with particle-mediated crystal growth. Mechanisms for conversion of ferrihydrite to the more stable phases range from dissolution of ferrihydrite followed by precipitation of the more stable phase as new nuclei or onto existing nuclei to aggregation-induced phase transformations. Elucidating these mechanisms is complicated by the limits of current characterization methods as well as our poor understanding of the nature of this ubiquitous material.

13.4 Outlook

Iron oxides are important players in the geochemical cycling of the elements as well as synthetic and naturally occurring chemical species. They can participate in redox reactions and can be exploited in remediation of contaminants in a wide range of settings. Particle size, morphology, composition, and microstructure on chemical behavior can all dramatically affect the chemical behavior of iron oxides. Furthermore, these materials are used in a wide range of industrial settings, magnetic recording media, water treatment facilities, pigments, and more. Thus, the importance of elucidating how the iron oxides form, transform, grow, and even dissolve is far reaching. Detailed examination of direct images of final crystals

has yielded dramatic insights into the mechanisms by which iron oxide crystals form, but reliance on such images is risky since features produced during the early stages of crystal growth can effectively be erased by later processes. Thus, the best approach combines a suite of time-resolved and in situ methods in order to elucidate the formation and growth history of the crystalline iron oxides. Elucidating the mechanisms by which iron oxides grow and transform in complex environments will require advancements in in situ materials characterization methods.

Acknowledgments We acknowledge the University of Minnesota, the National Science Foundation (No. NSF-0957696), and the Nanostructural Materials and Processes Program at the University of Minnesota for the financial support. We also thank Characterization Facility at the University of Minnesota, a member of the NSF-funded Materials Research Facilities Network (www.mrfn.org) via the MRSEC program (Figs. 13.2, 13.3, and 13.4). In addition, the TEM images shown in Fig. 13.5 were obtained using a Tecnai TF20 FEI microscope located at the Pacific Northwest National Laboratory, which is operated by Battelle Memorial Institute for the US Department of Energy under Contract DE-AC05-76RL01830.

References

Bailey JK, Brinker CJ, Mecartney ML (1993) Growth mechanisms of iron oxide particles of differing morphologies from the forced hydrolysis of ferric chloride solutions. J Colloid Interface Sci 157:1–13

Banfield JF, Welch SA, Zhang H, Thomsen Ebert T, Lee Penn R (2000) Aggregation-based crystal growth and microstructure development in natural iron oxyhydroxide biomineralization products. Science 289:751–754

Barker WW, Welch SA, Chu S, Banfield JF (1998) Experimental observations of the effects of bacteria on aluminosilicate weathering. Am Mineral 83:1551–1563

Barron V, Torrent J (2013) Iron, manganese and aluminium oxides and oxyhydroxides. Miner Nanoscale 14:297–336

Burleson DJ, Penn RL (2006) Two-step growth of goethite from ferrihydrite. Langmuir 22:402–409

Burrows ND, Penn RL (2013) Cryogenic transmission electron microscopy: aqueous suspensions of nanoscale objects. Microsc Microanal 19:1542–1553

Burrows ND, Yuwono VM, Penn RL (2010) Quantifying the kinetics of crystal growth by oriented aggregation. Mater Res Sci Bull 35:133–137

Burrows ND, Hale CRH, Penn RL (2012) Effect of ionic strength on the kinetics of crystal growth by oriented aggregation. Cryst Growth Des 12:4787–4797

Burrows ND, Hale CRH, Penn RL (2013) Effect of pH on the kinetics of crystal growth by oriented aggregation. Cryst Growth Des 13:3396–3403

Burrows ND, Kesselman E, Sabyrov K, Stemig A, Talmon Y, Penn RL (2014) Crystalline nanoparticle aggregation in non-aqueous solvents. CrystEngComm 16:1472–1481

Cao G (2004) Nanostructures and nanomaterials: synthesis, properties and applications. Imperial College Press, London

Chan CS, De Stasio G, Welch SA, Girasole M, Frazer BH, Nesterova MV, Fakra S, Banfield JF (2004) Microbial polysaccharides template assembly of nanocrystal fibers. Science 303:1656–1658

Chiche D, Digne M, Revel R, Chaneac C, Jolivet JP (2008) Accurate determination of oxide nanoparticle size and shape based on X-ray powder pattern simulation: application to boehmite AlOOH. J Phys Chem C 112:8524–8533

Cölfen H, Mann S (2003) Higher-order organization by mesoscale self-assembly and transformation of hybrid nanostructures. Angew Chem Int Ed 42:2350–2365
Cornell RM, Schwertmann U (2003) The iron oxides: structures, properties, reactions, occurrences and uses. Wiley-VCH, Weinheim
Cornell RM, Schwertmann U (2006) The iron oxides: structure, properties, reactions, occurrences and uses, 2nd, completely revised and extended edition. Wiley-VCH, Weinheim
Cornell RM, Schneider W, Giovanoli R (1989) Phase transformations in the ferrihydrite/cysteine system. Polyhedron 8:2829–2836
Dalmaschio CJ, Ribeiro C, Leite ER (2010) Impact of the colloidal state on the oriented attachment growth mechanism. Nanoscale 2:2336–2345
Davidson LE, Shaw S, Benning LG (2008) The kinetics and mechanisms of schwertmannite transformation to goethite and hematite under alkaline conditions. Am Mineral 93:1326–1337
Davis TM, Drews TO, Ramanan H, He C, Dong JS, Schnablegger H, Katsoulakis M, Kokkoli E, Mccormick A, Penn RL, Tsapatsis M (2006) Mechanistic principles of nanoparticle evolution to zeolite crystals. Nat Mater 5:400–408
De Yoreo JJ, Gilbert PUPA, Sommerdijk NAJM, Penn RL, Whitelam S, Joester D, Zhang HZ, Rimer JD, Navrotsky A, Banfield JF, Wallace AF, Michel FM, Meldrum FC, Cölfen H, Dove PM (2015) Toward a comprehensive picture of crystallization by particle attachment. doi: 10.1126/science.aaa6760
De Yoreo JJ, Sommerdijk NAJM, Dove PM (2017) Nucleation pathways in electrolyte solutions. In: Van Driessche AES, Kellermeier M, Benning LG, Gebauer D (eds) New perspectives on mineral nucleation and growth, Springer, Cham, pp 1–24
Drews TO, Tsapatsis M (2007) Model of the evolution of nanoparticles to crystals via an aggregative growth mechanism. Micropor Meospor Mater 101:97–107
Drits VA, Sakharov BA, Salyn AL, Manceau A (1993) Structural model for ferrihydrite. Clay Miner 28:185–207
Fischer WR, Schwertmann U (1975) The formation of hematite from amorphous iron(III) hydroxide. Clays Clay Miner 23:33–37
Frandsen C, Legg BA, Comolli LR, Zhang H, Gilbert B, Johnson E, Banfield JF (2014) Aggregation-induced growth and transformation of b-FeOOH nanorods to micron-sized a-Fe_2O_3 spindles. CrystEngComm 16:1451–1458
Gilbert B, Erbs JJ, Penn RL, Petkov V, Spagnoli D, Waychunas GA (2013) A disordered nanoparticle model for 6-line ferrihydrite. Am Mineral 98:1465–1476
Grogan JM, Schneider NM, Ross FM, Bau HH (2012) The nanoaquarium: a new paradigm in electron microscopy. J Indian Inst Sci 92:295–308
Hapiuk D, Masenelli B, Masenelli-Varlot K, Tainoff D, Boisron O, Albin C, Mélinon P (2013) Oriented attachment of ZnO nanocrystals. J Phys Chem C 117:10220–10227
Hochella MF Jr, Lower SK, Maurice PA, Penn RL, Sahai N, Sparks DL, Twining BS (2008) Nanominerals, mineral nanoparticles, and earth systems. Geochim Cosmochim Acta 72:A382
Huang F, Zhang HZ, Banfield J (2003) Two-stage crystal-growth kinetics observed during hydrothermal coarsening of nanocrystalline ZnS. Nano Lett 3:373–378
Ivanov VK, Fedorov PP, Baranchikov AY, Osiko VV (2014) Oriented attachment of particles: 100 years of investigations of non-classical crystal growth. Russ Chem Rev 83:1204–1222
Janney DE, Cowley JM, Buseck PR (2000) Structure of synthetic 2-line ferrihydrite by electron nanodiffraction. Am Mineral 85:1180–1187
Janney DE, Cowley JM, Buseck PR (2001) Structure of synthetic 6-line ferrihydrite by electron nanodiffraction. Am Mineral 86:327–335
Kandori K, Kawashima Y, Ishikawa T (1991) Characterization of monodispersed hematite particles by gas-adsorption and Fourier-transform infrared-spectroscopy. J Chem Soc Faraday Trans 87:2241–2246
Kumar S, Wang Z, Penn RL, Tsapatsis M (2008) A structural resolution cryo-TEM study of the early stages of MFI growth. J Am Chem Soc 130:17284–17286
Kumar S, Penn RL, Tsapatsis M (2011) On the nucleation and crystallization of silicalite-1 from a dilute clear sol. Micropor Mesopor Mater 144:74–81

Li D, Nielsen MH, Lee JR, Frandsen C, Banfield JF, De Yoreo JJ (2012) Direction-specific interactions control crystal growth by oriented attachment. Science 336:1014–1018

Liu Y, Lin XM, Sun Y, Rajh T (2013) In situ visualization of self-assembly of charged gold nanoparticles. J Am Chem Soc 135:3764–3767

Michel FM, Ehm L, Antao SM, Lee PL, Chupas PJ, Liu G, Strongin DR, Schoonen MAA, Phillips BL, Parise JB (2007) The structure of ferrihydrite, a nanocrystalline material. Science 316:1726–1729

Mintova S, Olson NH, Senker J, Bein T (2002) Mechanism of the transformation of silica precursor solutions into Si-MFI zeolite. Angew Chem Int Ed 41:2558–2561

Morales MP, Gonzalezcarreno T, Serna CJ (1992) The formation of alpha-Fe_2O_3 monodispersed particles in solution. J Mater Res 7:2538–2545

Murphy PJ, Posner AM, Quirk JP (1976a) Characterization of partially neutralized ferric nitrate solutions. J Colloid Interface Sci 56:270–283

Murphy PJ, Posner AM, Quirk JP (1976b) Characterization of partially neutralized ferric perchlorate solutions. J Colloid Interface Sci 56:298–311

Murphy PJ, Posner AM, Quirk JP (1976c) Characterization of partially neutralized ferric-chloride solutions. J Colloid Interface Sci 56:284–297

Navrotsky A (2011) Nanoscale effects on thermodynamics and phase equilibria in oxide systems. ChemPhysChem 12:2207–2215

Navrotsky A, Mazeina L, Majzlan J (2008) Size-driven structural and thermodynamic complexity in iron oxides. Science 319:1635–1638

Niederberger M, Cölfen H (2006) Oriented attachment and mesocrystals: non-classical crystallization mechanisms based on nanoparticle assembly. Phys Chem Chem Phys 8:3271–3287

Nielsen MH, De Yoreo JJ (2017) Liquid phase TEM investigations of crystal nucleation, growth, and transformation. In: Van Driessche AES, Kellermeier M, Benning LG, Gebauer D (eds) New perspectives on mineral nucleation and growth, Springer, Cham, pp 353–371

Ocaña M, Morales MP, Serna CJ (1995) The growth mechanism of a-Fe_2O_3 ellipsoidal particles in solution. J Colloid Interface Sci 171:85–91

Pan Y, Brown A, Brydson R, Warley A, Li A, Powell J (2006) Electron beam damage studies of synthetic 6-line ferrihydrite and ferritin molecule cores within a human liver biopsy. Micron 37:403–411

Penn RL (2004) Kinetics of oriented aggregation. J Phys Chem B 108:12707–12712

Penn RL, Soltis JA (2014) Characterizing crystal growth by oriented aggregation. CrystEngComm 16:1409–1418

Penn RL, Oskam G, Strathmann TJ, Searson PC, Stone AT, Veblen DR (2001a) Epitaxial assembly in aged colloids. J Phys Chem B 105:2177–2182

Penn RL, Zhu C, Xu H, Veblen DR (2001b) Iron oxide coatings on sand grains from the Atlantic coastal plain: high-resolution transmission electron microscopy characterization. Geology 29:843–846

Penn RL, Erbs J, Gulliver D (2006) Controlled growth of alpha-FeOOH nanorods by exploiting-oriented aggregation. J Cryst Growth 293:1–4

Penn RL, Tanaka K, Erbs J (2007) Size dependent kinetics of oriented aggregation. J Cryst Growth 309:97–102

Rao A, Cölfen H (2017) Mineralization schemes in the living world: mesocrystals. In: Van Driessche AES, Kellermeier M, Benning LG, Gebauer D (eds) New perspectives on mineral nucleation and growth, Springer, Cham, pp 155–184

Ross FM (2015) Opportunities and challenges in liquid cell electron microscopy. Science 350:aaa9886-1–aaa9886-9

Schwahn D, Ma Y, Cölfen H (2007) Mesocrystal to single crystal transformation of d, l-alanine evidenced by small angle neutron scattering. J Phys Chem C 111:3224–3227

Schwertmann U, Cornell RM (2000) Iron oxides in the laboratory: preparation and characterization. Wiley-VCH, Weinheim

Schwertmann U, Murad E (1983) Effect of pH on the formation of goethite and hematite from ferrihydrite. Clays Clay Miner 31:277–284

Shaw S, Pepper SE, Bryan ND, Livens FR (2005) The kinetics and mechanisms of goethite and hematite crystallization under alkaline conditions, and in the presence of phosphate. Am Mineral 90:1852–1860

Stawski TM, Benning LG (2013) SAXS in inorganic and bioinspired research. In: De Yoreo JJ (ed) Research methods in biomineralization science. Academic, San Diego

Sugimoto T, Muramatsu A, Sakata K, Shindo D (1993) Characterization of hematite particles of different shapes. J Colloid Interface Sci 158:420–428

Van der Zee C, Roberts DR, Rancourt DG, Slomp CP (2003) Nanogoethite is the dominant reactive oxyhydroxide phase in lake and marine sediments. Geology 31:993–996

Van Driessche AES, Benning LG, Rodriguez-Blanco JD, Ossorio M, Bots P, Garcia-Ruiz JM (2012) The role and implications of bassanite as a stable precursor phase to gypsum precipitation. Science 336:69–72

Watson JHL, Cardell RR Jr, Heller W (1962) The internal structure of colloidal crystals of beta-FeOOH and remarks on their assemblies in schiller layers. J Phys Chem 66:1757–1763

Waychunas GA, Kim CS, Banfield JF (2005) Nanoparticulate iron oxide minerals in soils and sediments: unique properties and contaminant scavenging mechanisms. J Nanopart Res 7:409–433

Xiong Y, Tang Z (2012) Role of self-assembly in construction of inorganic nanostructural materials. Sci China-Chem 55:2272–2282

Xue X, Penn RL, Leite ER, Huang F, Lin Z (2014) Crystal growth by oriented attachment: kinetic models and control factors. CrystEngComm 16:1419–1429

Yuk JM, Park J, Ercius P, Kim K, Hellebusch DJ, Crommie MF, Lee JY, Zettl A, Alivisatos AP (2012) High-resolution EM of colloidal nanocrystal growth using graphene liquid cells. Science 336:61–64

Yuwono V, Burrows ND, Soltis JA, Penn RL (2010) Oriented aggregation: formation and transformation of mesocrystal intermediates revealed. J Am Chem Soc 132:2163–2165

Yuwono VM, Burrows ND, Soltis JA, Do T, Penn RL (2012) Aggregation of ferrihydrite nanoparticles in aqueous systems. Faraday Discuss 159:235–245

Zhang Q, Liu S, Yu S (2009) Recent advances in oriented attachment growth and synthesis of functional materials: concept, evidence, mechanism, and future. J Mater Chem 19:191–207

Zhang J, Huang F, Lin Z (2010) Progress of nanocrystalline growth kinetics based on oriented attachment. Nanoscale 2:18–34

Zheng H, Smith RK, Jun YW, Kisielowski C, Dahmen U, Alivisatos AP (2009) Observation of single colloidal platinum nanocrystal growth trajectories. Science 324:1309–1312